



## Molecular Crystals and Liquid Crystals

Publication details, including instructions for authors and subscription information:

<http://www.tandfonline.com/loi/gmcl20>

## Visco-Elastic Properties of Nematic-MoS<sub>2</sub> Nanotubes Mixtures

M. Avsec<sup>a</sup>, A. Mertelj<sup>a</sup>, I. Drevensek-Olenik<sup>a</sup>, A. Mrzel<sup>a</sup> & M. Copic<sup>a</sup>

<sup>a</sup> Jozef Stefan Institute, Jamova, Ljubljana, Slovenia

Version of record first published: 31 Aug 2006

To cite this article: M. Avsec, A. Mertelj, I. Drevensek-Olenik, A. Mrzel & M. Copic (2005): Visco-Elastic Properties of Nematic-MoS<sub>2</sub> Nanotubes Mixtures, Molecular Crystals and Liquid Crystals, 435:1, 163/[823]-172/[832]

To link to this article: <http://dx.doi.org/10.1080/15421400590954506>

PLEASE SCROLL DOWN FOR ARTICLE

Full terms and conditions of use: <http://www.tandfonline.com/page/terms-and-conditions>

This article may be used for research, teaching, and private study purposes. Any substantial or systematic reproduction, redistribution, reselling, loan, sub-licensing, systematic supply, or distribution in any form to anyone is expressly forbidden.

The publisher does not give any warranty express or implied or make any representation that the contents will be complete or accurate or up to date. The accuracy of any instructions, formulae, and drug doses should be independently verified with primary sources. The publisher shall not be liable for any loss, actions, claims, proceedings, demand, or costs or damages

whatsoever or howsoever caused arising directly or indirectly in connection with or arising out of the use of this material.



## Visco-Elastic Properties of Nematic-MoS<sub>2</sub> Nanotubes Mixtures

M. Avsec

A. Mertelj

I. Drevensek-Olenik

A. Mrzel

M. Copic

Jozef Stefan Institute, Jamova, Ljubljana, Slovenia

*We investigated experimentally the viscoelastic properties of MoS<sub>2</sub> nanotubes mixed with liquid crystal 8CB in the nematic phase. The MoS<sub>2</sub> nanotubes were dispersed with ultra-sound in ethanol and then mixed with liquid crystal; then the ethanol was evaporated. Dynamic light scattering (DLS) was used to measure the viscoelastic coefficients of the mixture in its nematic phase from the SmA-N up to the N-I phase transition. The relaxation time  $\tau$  of orientational fluctuations depends on the concentration of dispersed MoS<sub>2</sub> nanotubes in liquid crystal, temperature and orientation of the director. By measuring the dependence of  $\tau$  as a function of the scattering wave vector  $\mathbf{q}$ , the ratio  $K_1/\eta_1$  and  $K_3/\eta_3$  were obtained ( $K_i$  - Frank elastic constants,  $\eta_i$  - effective viscosities). Comparison of the obtained results with the values of  $K_i/\eta_i$  of pure 8CB liquid crystal shows that the ratios  $K_1/\eta_1$  and  $K_3/\eta_3$  decrease with increasing concentration of the MoS<sub>2</sub> nanotubes.*

**Keywords:** alignment; dynamic light scattering; liquid crystal; mixture; nanotubes; orientational fluctuations

### 1. INTRODUCTION

The discovery of free-standing microscopic one-dimensional molecular structures, such as molybdenum disulfide nanotubes, has attracted recently a lot of attention due to various interesting properties associated with their small dimensions, high anisotropy, and intriguing tube-like structures. The recent studies performed on them implicate a variety of different. Their investigations studies of a variety of

Address correspondence to M. Avsec, Jozef Stefan Institute, Jamova 39, 1001 Ljubljana, Slovenia. E-mail: matija.acsec@ijs.si

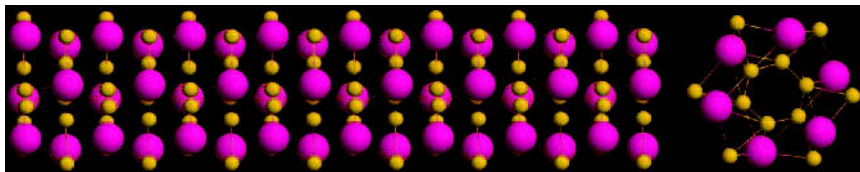


**FIGURE 1** Structure of the subnanometer-diameter monomolecular  $\text{MoS}_2$  single-wall nanotubes. The bundles consist from hexagonal close-packed sulfur-molybdenum-sulfur cylinders (● Mo, · S).

quantum effects [6,7] to potentially useful properties such as efficient field emission [8] and exceptional mechanical strength [9]. The structural properties of  $\text{MoS}_2$  nanotubes have been the subject of extensive theoretical calculations, which have predicted conditions for their stability in cylindrical form and some interesting electronic properties [1,2]. The spontaneous alignment and self-assembly of the  $\text{MoS}_2$  nanotubes, the tip geometry, and the porous structure place this new compound among the important materials for advanced electronics, for nanodevices and, for storage containers.

The aim of this work was to investigate the  $\text{MoS}_2$  nanotubes and narrow bundles decomposed from wide bundles, which generally show a strong tendency for self- or hetero-assembly. Typically, they are attracted by the surface steps or by the crystal edges of the substrate, so addition nanotubes or narrow bundles produce a large distortion of the growth direction. We tried to solve this problem and to obtain oriented samples by aligning them in a mixture with the 8CB liquid crystal in its nematic phase. Since the chemically treated  $\text{MoS}_2$  nanotubes exhibit metallic behavior we believe they are a possible candidate for the one-dimensional molecular wires.

We report on the fluctuation relaxation time  $\tau$  and viscoelastic properties of the 8CB- $\text{MoS}_2$  nanotubes mixtures, probed by dynamic light scattering (DLS) method. We presume that the  $\text{MoS}_2$  tubes in the mixture had a subnanometer-diameter and a monomolecular single-wall structure (Fig. 1).

## 2. PREPARATION OF THE SAMPLE

The single-wall  $\text{MoS}_2$  nanotubes were produced by a catalyzed transport method using  $\text{C}_{60}$  as a growth promoter in the reaction [1]. The transported material grows in the form of bundles oriented perpendicular to the substrate surface (Fig. 2a), consisting of individual  $\text{MoS}_2$  nanotubes. These bundles start to grow from randomly

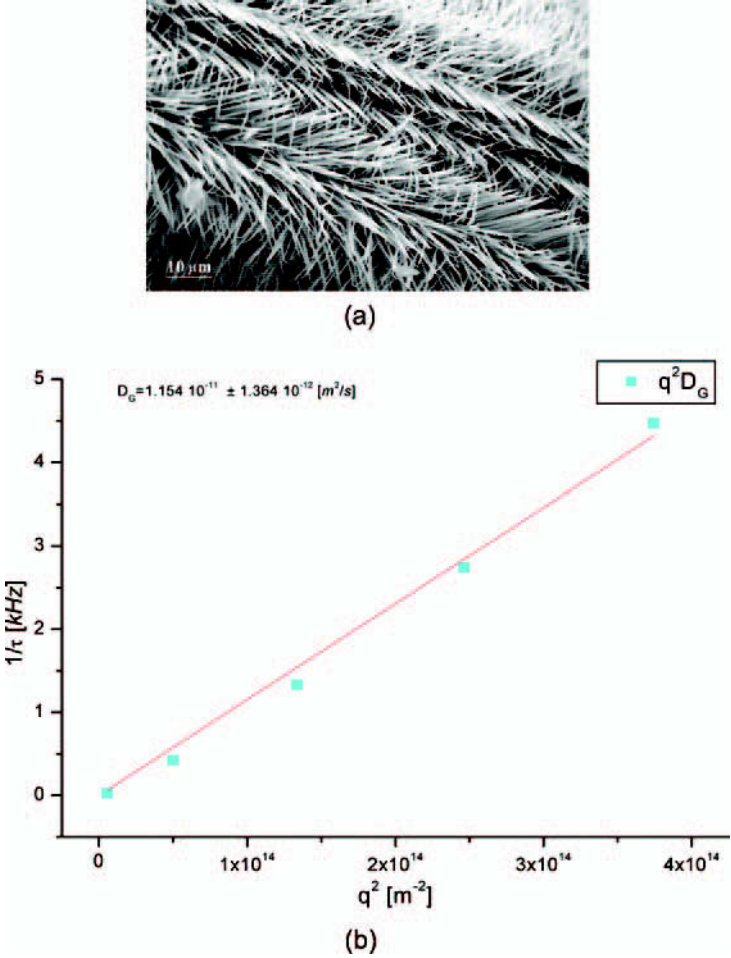


**FIGURE 2** (a) Scanning electron image. Bundles appear to self-assemble into sharp points on the end. (b) Inverse relaxation time of the polarized mode versus square of the scattering vector. Calculated translational and rotational diffusion coefficients are:  $D_G \approx 1.15 \cdot 10^{-11} [m^2/s]$  and  $D_r \approx 69700 [s^{-1}]$  respectively.

distributed nucleation sites on the quartz surface. The bundles usually terminate in a sharp tip, forming sharp needles, with each bundle containing  $> 5 \cdot 10^5$  ordered nanotubes. The secondary nucleation of the bundles on the rough top surface leads to the formation of microscopic geometrical shapes (Fig. 2a). Examination of the bundles by SEM reveals the presence of the parallel grown strands. These strands were

disassembled into thinner ones and even individual tubes by dispersion in ethanol using ultrasound.

The 0.1 mg of MoS<sub>2</sub> bundles powder was added to 40 ml ethanol and the solution was typically put for 6 hours in the ultrasound bath. After this, the solution was filtered by 200 nm pore size filter. The average size of dispersed bundles in the dilute solution was deduced with the dynamic light scattering method (DLS). The high-resolution transmission electron microscopy data (HRTEM) show that the bundles have a cylindrical form [1]. Because of these we use the hydrodynamic- diffusion theory for rigid rods to analyze the two independent kinds of Brownian motion, i.e., translational and rotational [10]. The rotational diffusion constant  $D_r$  was computed from the Kirkwood-diffusion theory [10]

$$D_r = \frac{3k_B T [\ln(L/b) - \gamma]}{\pi \eta_s L^3}, \quad (1)$$

where  $L$  and  $b$  are average length and diameter of the bundles,  $\gamma = 0.8$  is a correction factor [10] and  $\eta_s$  is the viscosity of ethanol. The translational diffusion constant for long cylinders ( $L > 3b$ ) is given by [10]

$$D_G = \frac{\ln(L/b)}{3\pi \eta_s L} k_B T. \quad (2)$$

For selected scattering geometry where the polarizer and analyzers select out the components of the scattered electric field we measured the autocorrelation function of the scattered light intensity for different scattering wave vectors  $\mathbf{q}$  and for two different polarization directions of the scattered light. When the polarizer and analyzers were parallel, the polarized  $I_{VV}^{(1)}$  scattered intensity in the heterodyne regime was measured which is proportional to

$$I_{VV}^{(1)} = A_1 e^{-q^2 D_G t} + B_1 e^{-(6D_r + q^2 D_G)t}, \quad (3)$$

where the  $A_1$  and  $B_1$  are the polarizability parameters [4]. When the polarizer and analyzers were perpendicular depolarized intensity  $I_{VH}^{(1)}$  was measured

$$I_{VH}^{(1)} = \frac{3}{4} B_1 e^{-(6D_r + q^2 D_G)t}. \quad (4)$$

Since nanotubes have large optical anisotropy, they produce significant depolarized light scattering. From the measured DLS intensities  $I_{VV}^{(1)}$  and  $I_{VH}^{(1)}$  combined with equations 1 and 2 average rotational and translational diffusion coefficients were determined (Fig. 2b). Appropriate

length and diameter of cylindrical bundles in the dilute solution was found to be  $L = 17 \text{ nm} \pm 4 \text{ nm}$  and  $b = 6 \text{ nm} \pm 1.5 \text{ nm}$ .  $\text{MoS}_2$  bundles dispersed in ethanol were then mixed with 8CB liquid crystal; after this ethanol was evaporated. In order to probe orientational fluctuations a planar cell was filled with the mixture using two glass plates with rubbed polymer substrates. The direction of molecules in the nematic phase was parallel with preferred direction of the rubbed planar cell. The thickness of the cell was  $100 \mu\text{m}$ .

### 3. DETERMINATION OF VISCOELASTIC PROPERTIES BY LIGHT SCATTERING

The thermally excited director fluctuations give rise to fluctuations of the optical dielectric tensor which cause strong scattering of light [2]. For a given scattering wave vector  $\mathbf{q}$ , the scattered-light amplitude depends on two independent Fourier components  $n_1(\mathbf{q})$  and  $n_2(\mathbf{q})$  of the director fluctuation  $\delta\mathbf{n}$  [3], which correspond to the components along the axes of the coordinate system defined as

$$\mathbf{e}_3 \parallel \mathbf{n}, \mathbf{e}_2 = \frac{\mathbf{e}_3 \times \mathbf{q}}{|\mathbf{e}_3 \times \mathbf{q}|} \quad \text{and} \quad \mathbf{e}_1 = \mathbf{e}_2 \times \mathbf{e}_3. \quad (5)$$

In this coordinate system, the scattering wave vector lies in  $(\mathbf{e}_1, \mathbf{e}_2)$  plane and can be written as  $\mathbf{q} = (q_1, 0, q_3) = (q_\perp, 0, q_\parallel)$ . The first component of the director fluctuation  $n_1(\mathbf{q})$  corresponds to the splay-bend and the second  $n_2(\mathbf{q})$  to the twist-bend mode. The relaxation times of these modes are given as

$$\frac{1}{\tau_\beta(\mathbf{q})} = \frac{K_\beta q_\perp^2 + K_3 q_\parallel^2}{\eta_\beta(\mathbf{q})}, \quad (6)$$

where  $\beta = 1, 2$ ,

$$\eta_1(\mathbf{q}) = \gamma_1 - \frac{(q_\perp^2 \mu_3 - q_\parallel^2 \mu_2)^2}{q_\perp^4 \eta_b + q_\perp^2 q_\parallel^2 (\mu_1 + \mu_3 + \mu_4 + \mu_5) + q_\parallel^4 \eta_c}$$

and

$$\eta_2(\mathbf{q}) = \gamma_1 - \frac{q_\parallel^2 \mu_2^2}{q_\perp^2 \eta_a + q_\parallel^2 \eta_c},$$

where  $\mu_i$  are Leslie viscosity coefficients,  $\eta_a$ ,  $\eta_b$  and  $\eta_c$  Miesowicz viscosities and  $K_i$  Frank elastic constants.

The homodyne light intensity autocorrelation function  $g^{(2)}(\mathbf{q}, t') = \langle I(t' + \tau) \cdot I(t') \rangle$  of the scattered light in the nematic liquid crystal is associated with the field autocorrelation function of the Fourier components of the director orientation fluctuation  $G^{(1)}(\mathbf{q}, t') = \langle \mathbf{E}(t' + \tau) \cdot \mathbf{E}(t') \rangle$ :

$$g^{(2)}(\mathbf{q}, t) = 1 + \frac{|G^{(1)}(\mathbf{q}, t)|}{I_D^2}, \quad (7)$$

where

$$G^{(1)}(\mathbf{q}, t) = A \sum_{\beta=1}^2 \frac{S_{\beta}^2(\mathbf{q})}{K_{\beta} q_{\perp}^2 + K_3 q_{\parallel}^2} \cdot e^{-\frac{t}{2\tau_{\beta}(\mathbf{q})}}.$$

The geometrical factor  $S_{\beta}$  depends on the polarizations of incident (i) and scattered light (f)

$$S_{\beta} = \mathbf{f} \cdot (\mathbf{e}_3 \otimes \mathbf{e}_{\beta} + \mathbf{e}_{\beta} \otimes \mathbf{e}_3) \cdot \mathbf{i}, \quad (8)$$

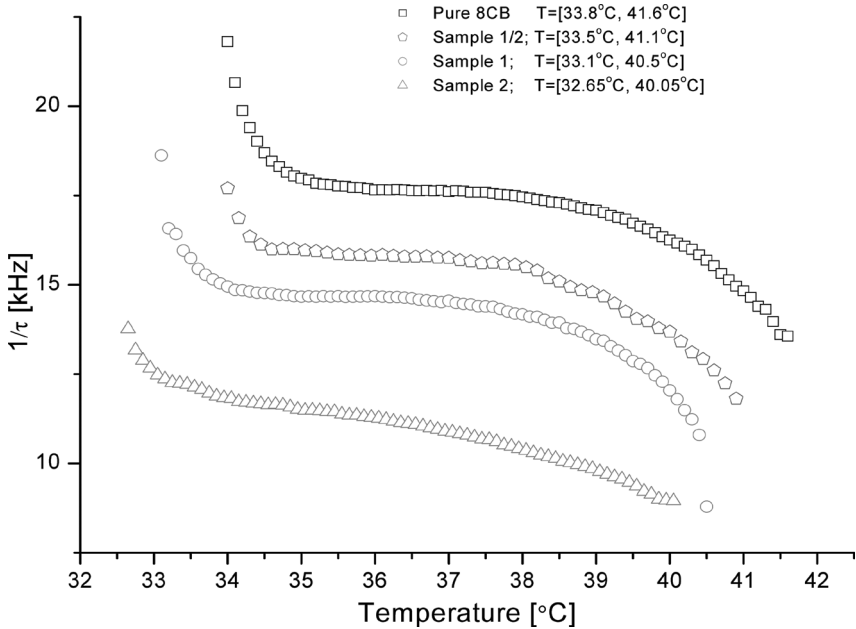


**FIGURE 3** Temperature dependence of the inverse relaxation time  $1/\tau_2$  for different concentrations of MoS<sub>2</sub>-bundles in the LC mixture measured at scattering angle  $\alpha = 50^\circ$ .



**TABLE 1** The Measured Results

Sample	Volume of MoS <sub>2</sub> + ethanol “mixed with 0.1 [ml] 8CB”	$K_3/\eta_3$	$K_1/\eta_1$
Pure 8CB		$2.56\cdot10^{-13}$ [m <sup>2</sup> /ms]	$8.555\cdot10^{-14}$ [m <sup>2</sup> /ms]
Sample 1/2	1/2 [ml]	$2.33\cdot10^{-13}$ [m <sup>2</sup> /ms]	$8.03\cdot10^{-14}$ [m <sup>2</sup> /ms]
Sample 1	1 [ml]	$2.18\cdot10^{-13}$ [m <sup>2</sup> /ms]	$7.64\cdot10^{-14}$ [m <sup>2</sup> /ms]
Sample 2	2 [ml]	$1.757\cdot10^{-13}$ [m <sup>2</sup> /ms]	$6.65\cdot10^{-14}$ [m <sup>2</sup> /ms]
Sample 3	3 [ml]	$1.185\cdot10^{-13}$ [m <sup>2</sup> /ms]	$5.599\cdot10^{-14}$ [m <sup>2</sup> /ms]

and the constant  $A$  depends on the temperature and the experimental setup.

In order to probe pure bend mode, i. e., to measure the value of the  $K_3/\eta_3$  where is  $\eta_3 = \eta_2(q_{\perp} \ll q_{\parallel})$  (Eq. 6), depolarized scattering geometry was used with incident beam polarized as extraordinary and scattered beam as ordinary beam (e-o). In this geometry the scattered plane was  $xz$ -plane of the laboratory frame and the direction of  $\mathbf{n}$

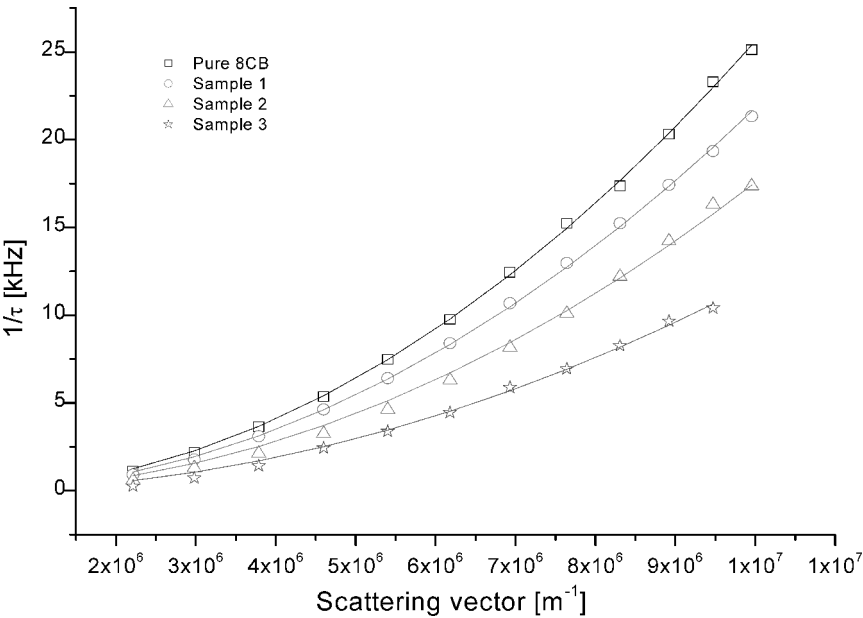


**FIGURE 4** Dependence of the inverse relaxation time  $1/\tau_2$  on the scattering wave vector  $\mathbf{q}$  measured for different concentrations of MoS<sub>2</sub>-bundles in the LC mixture.

was chosen in such way that  $q_{\perp} \ll q_{\parallel}$ . The inverse relaxation time  $1/\tau_2$  as a function of temperature for samples with different concentrations of  $\text{MoS}_2$  bundles is shown in Figure 3.

Far from the  $S_A$ -N transition the temperature behavior of the  $1/\tau_2 \propto K_3/\eta_3$  ( $q_{\parallel} = \text{constant}$ ) is typical for nematics, whereas near the  $S_A$ -N transition a clear divergence is observed, indicating the existence of the pretransitional smectic-like ordering in the nematic phase. Figure 3 shows that the ration  $K_3/\eta_3$  decreases by increasing concentration of the  $\text{MoS}_2$  (Table 1). Similar results were obtained also when we measured the dependence of the  $K_3/\eta_3$  on the scattering wave vector  $\mathbf{q}$  (Fig. 4).

The values of  $K_3/\eta_3$  measured for different concentrations are shown in Table 1, indicating the concentration dependence within the nematic range of  $\text{MoS}_2$  mixture.

The ratio  $K_1/\eta_1$  where  $\eta_1 = \eta_1(q_{\parallel} \ll q_{\perp})$  (Eq. 6) was obtained by using the scattering geometry associated to the splay deformation, which was performed, similar as in first case, by rotation of the sample cell (Fig. 5).

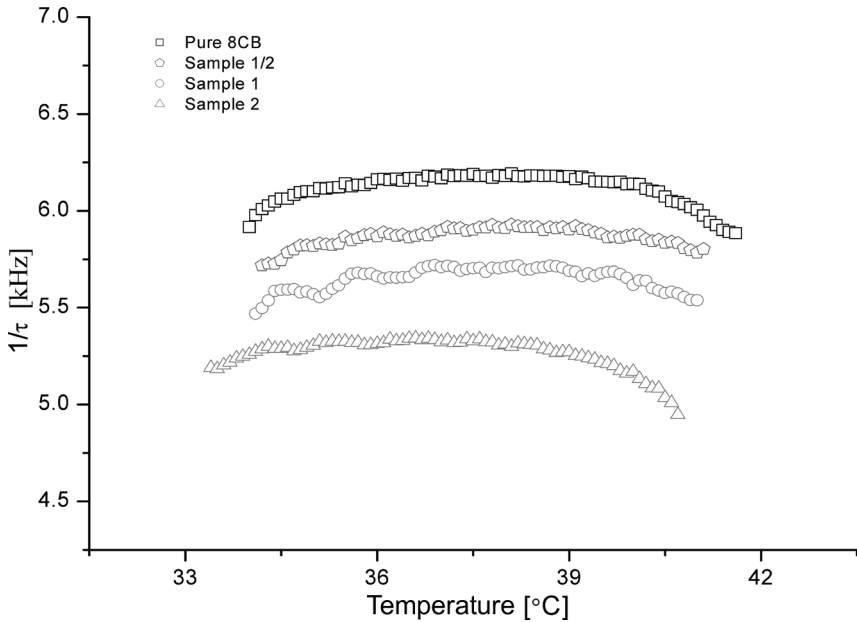


**FIGURE 5** Temperature dependence of the inverse relaxation time  $1/\tau_1$  for different concentrations of  $\text{MoS}_2$ -bundles in the LC mixture measured at scattering angle  $\alpha = 50^\circ$ .

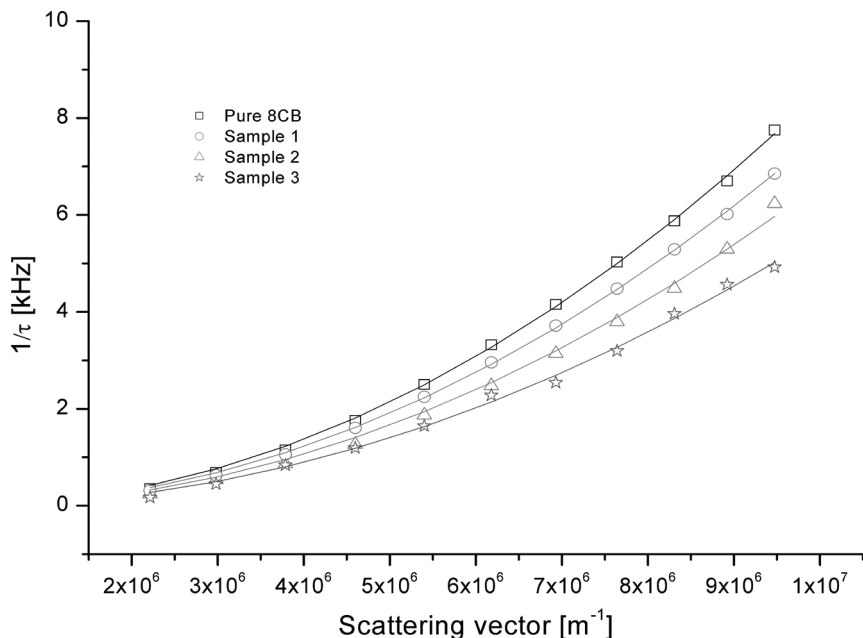


**FIGURE 6** Dependence of the inverse relaxation time  $1/\tau_1$  on the scattering wave vector  $\mathbf{q}$  measured for different concentrations of  $\text{MoS}_2$ -bundles in the LC mixture.

According to the data shown in Figure 5, the  $1/\tau_1 \propto K_1/\eta_1(\mathbf{q})$  ( $q_\perp = \text{constant}$ ,  $q_\parallel \approx 0$ ) undergoes a slight decrease near the  $S_A$ -N transition. The dependency of  $K_1/\eta_1$  on the scattering wave vector (Fig. 6) are in good agreement with those previously shown in Figure 5. (Table1)

#### 4. CONCLUSION

The major source for the decrease of  $K_1/\eta_1$  and  $K_3/\eta_3$  with increasing concentration of  $\text{MoS}_2$  bundles is in our opinion the increase of the viscous coefficients of director fluctuations due to the presence of higher concentration of the  $\text{MoS}_2$  bundles in the mixture. The results given in the Table 1 clearly indicate that viscoelastic properties of mixture were changed so confirming that some  $\text{MoS}_2$  bundles were dissolved in the liquid crystal.

Due to the large molecular anisotropy of  $\text{MoS}_2$  nanotubes, bundles can be oriented by an external field. Therefore electric or magnetic birefringence can be used as a practical tool to study the rotational motion of these nanotubes. DLS technique can be combined with the

analysis of fluctuation modes with optical polarization microscopy, which allowed us to determine the ratio  $K_3/K_1$ . With the combination of the two methods, one can determine the elastic constants  $K_1$ ,  $K_3$  and effective viscosities of the nematic-MoS<sub>2</sub> nanotubes mixture.

## REFERENCES

- [1] Remskar, M., Mrzel, A., Skraba, Z., Jesih, A., Ceh, M., Demsar, J. *et al.* (2001). *Science*, 292, 479.
- [2] Mertelj, A. & Copic, M. (1996). *Mol. Cryst. Liq. Cryst.*, 282, 35.
- [3] de Gennes, P. G. (1995). *The Physics of Liquid Crystal*, Clarendon Press: Oxford.
- [4] Berne, B. J. (2000). *Dynamic Light Scattering*, Wiley & Sons: New York.
- [5] Arcon, D. *et al.* (2003). *Phys. Rev. B*, 67, 125423.
- [6] Bockrath, M. *et al.* (1999). *Nature*, 397, 598.
- [7] Bockrath, M. *et al.* (1999). *Nature*, 389, 582.
- [8] de Heer, W. A., Chatelain, A., & Ugarte, D. (1995). *Science*, 270, 1179.
- [9] Treacy, M. M. J., Ebbesen, T. W., & Gibson, J. M. (1996). *Nature*, 381, 678.
- [10] Doi, M. (1986). *The Theory of Polymer Dynamics*, Clarendon Press: Oxford.
- [11] Mertelj, A., Jakli, A., & Copic, M. (1999). *Mol. Cryst. Liq. Cryst.*, 331, 81.
- [12] Mihailovic, D., Jaglicic, Z., Arcon, D., Mrzel, A., Zorko, A., Kabanov, V. V. *et al.* (2003). *Phys. Rev. Lett.*, 90, 146401.
- [13] Remskar, M., Mrzel, A. *et al.* (2003). *Adv. Mater.*, 15(3), 237.